ELSEVIER

International Journal of Mass Spectrometry 193 (1999) 69–75

International Journal of Mass Spectrometry

Resonant laser mass spectrometry: fragmentation patterns from $^{13}C_1$ naturally labeled molecules

John G. Philis*, Constantine Kosmidis

Department of Physics, University of Ioannina, GR45110 Ioannina, Greece

Received 10 May 1999; accepted 26 July 1999

Abstract

The potential of resonance-enhanced multiphoton ionization (REMPI) mass spectrometry to pick out the fragmentation pattern due to $^{13}C_1$-isotopomers from the fragmentation pattern due to the unlabeled molecule, in non-isotope-enriched samples, has been explored. Toluene, *n*-propylbenzene, *ortho*-diethylbenzene, and *tert*-butylbenzene have been used as testing samples. The fragmentation patterns of the unlabeled molecule and of the natural abundance $^{13}C_1$-isotopomer have been measured in a time-of-flight mass analyzer by exciting successively the $S_1 \leftarrow S_0$ origins of the ^{12}C-monoisotopic molecule and $^{13}C_1$-isotopomers. Fragmentation mechanisms are not completely clear from the comparison of these mass spectra, but the method can be applied to low concentration enriched compounds labeled in known positions. (Int J Mass Spectrom 193 (1999) 69–75) © 1999 Elsevier Science B.V.

Keywords: Laser mass spectrometry; Natural isotopic mixture; Alkylbenzenes; ^{13}C; REMPI

1. Introduction

Mass spectroscopy by multiphoton ionization (MPI) has been rapidly developed since 1978 [1–11]. The most effective and easiest scheme is when the molecule absorbs one UV photon in resonance to an intermediate excited energy level (e.g., S_1 origin) and absorption of a second photon leads the molecule above its ionization limit. The abbreviation R2PI is used for this (1 + 1) resonance ionization mechanism.

The special feature of resonance-enhanced multiphoton ionization (REMPI), as compared to other ionization techniques, is the wavelength selectivity of this method [1–17]. The wavelength selectivity becomes very high when a supersonic molecular beam is used. In a mixture of molecules, the component, which is preferentially ionized, is that whose absorption band is in resonance with the laser wavelength; therefore, a trace material can be detected. Isotope selectivity is an example-application of resonant laser mass spectrometry. This selectivity is based on isotopic shifts in molecular vibronic transitions. Boesl et al. [13] demonstrated that the $^{13}C_1$-benzene isotopomer can be preferentially ionized in a natural isotopic mixture by shifting the wavenumber by +1.6 cm^{-1} from the $S_1 6^1$ absorption band of C_6H_6. $^{13}C_1$ selectivity has been demonstrated in simple benzene derivatives: *p*-xylene toluene, fluorobenzene, and aniline [10,11,18,19]. Furthermore, Lubman et al. [20] studied the selective ionization of chlorine and bro-

* Corresponding author. E-mail: iphilis@cc.uoi.gr

PII S1387-3806(99)00152-9

mine isotopes in aromatic molecules. In all these studies on isotope selectivity, the intensity of the laser beam has been kept low, leading to the formation of parent ions only (soft ionization). Besides the wavelength selectivity, REMPI has the following characteristic: by increasing the laser intensity, different degrees of fragmentation can be reached, because the molecular cation absorbs additional photons and undergoes substantial fragmentation (partially hard ionization and very hard ionization). The "ladder switching model" via the molecular parent ion proposed by Schlag and co-workers [6,21] seems to be the typical mechanism for nanosecond excitation of most organic molecules.

Taking into consideration that by resonant laser mass spectrometry isotopic selectivity is feasible and that chemical synthesis of isotopically labeled molecules is an expensive and time-consuming process, we explore the possibility of measuring the fragmentation pattern of $^{13}C_1$-isotopomers, using an isotopically non-enriched sample. Specifically, in this communication, we present and discuss the fragmentation patterns recorded successively by selecting the appropriate laser wavelength: one corresponding to the unlabeled ^{12}C-molecule and one corresponding to the $^{13}C_1$-molecule. Toluene, *n*-propylbenzene, *ortho*-diethylbenzene, and *tert*-butylbenzene have been chosen for this presentation. Toluene is among the key molecules in the history of mass spectrometry because it generates the seven-membered-ring tropylium ion, $C_7H_7^+$ [22–24]. *n*-Propylbenzene is a medium sized alkylbenzene, while *ortho*-diethylbenzene and *tert*-butylbenzene are two structural isomers. The electron impact (EI) mass spectra can be found in [25].

2. Experimental

The experimental setup has been described elsewhere [26,27] and only the main procedure will be presented. Each sample, seeded in Ar or He (3 atm), expands into a vacuum chamber through a 0.5-mm-diameter pulsed valve. No skimmer is used in the present apparatus and the optimum conditions for exciting the coldest part of the molecular beam have been achieved by minimizing the valve-laser pulse delay so that the laser interacts with the top of the rising edge of the molecular beam pulse. Under these conditions the signal is not the strongest one, but the isotope enrichment factor within the photoions is maximum.

The UV laser light (BBO-I crystal, Lambda Physic LPD 3000 dye laser pumped by an excimer laser) is focused by an $f = +50$ cm lens at ~4.5 cm downstream from the valve exit. The laser intensity is of the order of 30 μJ/pulse and the pulse duration is ~6 ns.

The axis of the linear time-of-flight (TOF) mass analyzer is vertical to the laser beam and to the molecular beam. Ions formed by R2PI are transferred into the field-free region ($L = 1.17$ cm) after a two-step acceleration through the electrostatic fields $E_1 \approx 150$ V/cm (draw-out field) and $E_2 \approx 1600$ V/cm (main acceleration field). TOF mass spectra were accumulated and averaged over 256 laser shots by connecting the ion detector output through a fast preamplifier to a digitizing storage oscilloscope.

The samples are from Aldrich Chemical Co. and have been used without any further purification or isotopic enrichment.

3. Results and discussion

The R2PI mass selected $S_1 \leftarrow S_0$ origin band of the ^{12}C-monoisotopic and $^{13}C_1$-substituted molecule has been measured for each natural-abundance sample. These absorption spectra have been recorded by setting the gate of a BOX-CAR integrator on the corresponding parent-ion peak (time-of-flight mass analyzed spectrum). Next, the laser induced dissociation pattern was registered in the TOF analyzer at selected wavelengths: λ_{12}, the wavelength where the unlabeled molecule has maximum absorption and λ_{13}, the wavelength where the $^{13}C_1$ isotopomer has maximum absorption. For these two successive mass spectra, the laser intensity or other experimental parameters have been kept the same.

Wavelength λ_{13} is ~0.03 nm lower than λ_{12}, and a typical value of λ_{12} is in the range of 266 nm. The broadness of each origin band is due to the rotational

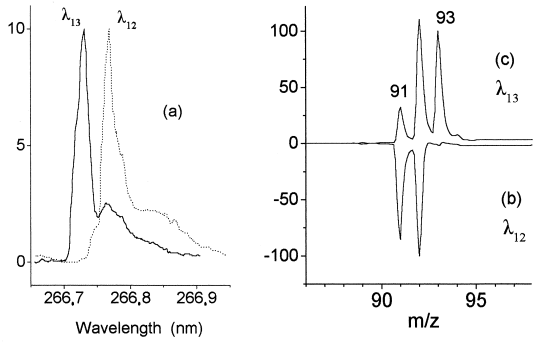

Fig. 1. (a) R2PI mass selected $S_1 \leftarrow S_0$ origin band of jet-cooled toluene (dotted line) and $^{13}C_1$-toluene (solid line). Both spectra have been scaled to 10. (b) REMPI mass spectrum of toluene induced by wavelength λ_{12}. (c) REMPI mass spectrum of toluene induced by wavelength λ_{13}. A non-isotope-enriched sample has been used and the parent peaks $C_7H_8^+$ in (b) and $^{13}CC_6H_8^+$ in (c) have been normalized to 100.

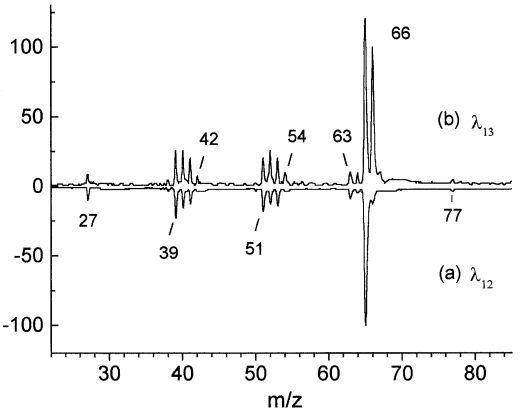

Fig. 2. REMPI mass spectra (lighter fragments) of toluene recorded with (a) laser wavelength tuned at λ_{12}, (b) laser wavelength tuned at λ_{13}.

structure, and the isotope selectivity is improved by increasing the cooling of the molecular beam. By adjusting the pressure of the carrier gas and the pulse duration of the jet valve, as well as the delay between laser firing and valve pulse, the rotational temperature was low enough to achieve isotope selectivity. Since no skimmer was involved in the apparatus, warmer molecules, which are outside of the central axis of the molecular beam, may contribute to the mass spectrum and therefore the separation factor of the process can be reduced. This effect is observable in the case of toluene because of its high absorption cross section, while for the other molecules it is unimportant.

In the discussion of the fragmentation patterns that follows, the isotopic scrambling, as is known from electron impact studies [24], is assumed because there is no reason to exempt this effect in the ladder switching model with laser pulses of nanosecond duration.

3.1. Toluene

In Fig. 1(a) the $S_1 \leftarrow S_0$ origin band of toluene and its $^{13}C_1$ isotopomer are displayed, both normalized to 10. The absorption coefficient of $^{13}CC_6H_8$ is maximum at $\lambda_{13} = 266.74$ nm, blue-shifted by $\sim$4 cm^{-1} relative to the $\lambda_{12} = 266.77$ nm absorption peak of toluene (C_7H_8). In $^{13}CC_6H_8$, the ^{13}C atom may be a ring carbon or the methyl carbon (distribution 6:1). Taking into consideration that the $S_1 \leftarrow S_0$ transition is a $\pi - \pi^*$ transition of the ring system, it is expected that the [ring-$^{13}C_1$] toluene will have a larger isotope shift than the [α-$^{13}C_1$] methyl group toluene and therefore the former, $^{13}CC_5H_5CH_3$, is preferentially excited at λ_{13}. This wavelength selectivity holds also for the other alkylbenzenes and is clearly seen in *tert*-butylbenzene.

Figs. 1(b), 1(c), and 2 show the mass spectra induced by R2PI at laser wavelengths λ_{12} and λ_{13}. In Fig. 1(b) and 1(c) the parent peaks [*m/z* 92 in Fig. 1(b) and *m/z* 93 in Fig. 1(c)] have been scaled to 100. In Fig. 2 the peak at *m/z* 65 [mass spectrum (a)] and the peak at *m/z* 66 [mass spectrum (b)] have been scaled to 100.

Fig. 1(b) shows that the contribution of $^{13}CC_6H_8^{\cdot+}$, *m/z* 93, is negligible at the wavelength λ_{12}, and the intensity of the *m/z* 91 ($C_7H_7^+$) fragment is strong because we are working in the REMPI hard ionization regime. The lower mass fragments of ^{12}C-toluene are displayed in Fig. 2(a) and only $^{12}C_yH_x^+$ ions are present. The interpretation is known from EI studies [22–24] and the main sequence is

$$\begin{array}{cccccccc} & & -H & & -C_2H_2 & & -C_2H_2 & \\ & C_7H_8^{\cdot+} & \rightarrow & C_7H_7^{+} & \rightarrow & C_5H_5^{+} & \rightarrow & C_3H_3^{+} \\ m/z & 92 & & 91 & & 65 & & 39 \end{array} \quad (1)$$

In Fig. 2 the *m/z* 38, 50, and 63 fragments are weak, contrary to the EI pattern. By increasing the laser pulse energy, the $C_3H_x^+$ and $C_4H_x^+$ ($x = 2–5$) peaks as well as the $C_2H_3^+$ peak gain intensity relative to the $C_5H_5^+$ and the parent peak. This behavior is due to the ladder switching model for multiphoton ionization, and it seems that Eq. (1) is valid for this process, too. The *m/z* 77 fragment $C_6H_5^+$ is as weak as in the EI mass spectrum. Very weak peaks are also detectable at *m/z* 89 and 90 [Figs. 1(b), 1(c)].

By tuning the laser wavelength to λ_{13}, the ion current due to $^{13}CC_6H_8^+$ and its fragments increases, while the current due to $C_7H_8^+$ and its fragments decreases (Figs. 1(c), 1(b), and 2). Now the *m/z* 92 peak is a mixture of $C_7H_8^{\cdot+}$ (toluene cation) and of the fragment $^{13}CC_6H_7^+$, while the *m/z* 91 peak is due to the $C_7H_7^+$ fragment from $C_7H_8^{\cdot+}$. The fragments of lower mass are displayed in Fig. 2(b). The *m/z* 66 peak is a composition of $^{13}CC_4H_5^+$ and $C_5H_6^+$. The former ion is the major component, formed from $^{13}CC_6H_7^+$ by the elimination of C_2H_2 (Eq. 1), while the ion $C_5H_6^+$ comes from monoisotopic toluene. Expulsion of $^{13}CCH_2$ from $^{13}CC_6H_7^+$ yields $C_5H_5^+$, which contributes to the *m/z* 65 peak. $C_5H_5^+$ has been also produced from $C_7H_7^+$ by elimination of C_2H_2. Taking into consideration the relative intensity of the peaks, we estimate that the $^{13}CC_6H_8$ concentration is ~55% within the photoions. The influence of wavelength isotope selectivity is also seen in the region around *m/z* 39 (fragments $C_3H_x^+$) and *m/z* 51 (fragments $C_4H_x^+$). The *m/z* 77 fragment ($C_6H_5^+$) is still detectable with λ_{13} R2PI, but the $^{13}CC_5H_5^+$ peak (*m/z* 78) is not seen clearly.

3.2. n-Propylbenzene

$C_6H_5C_3H_7$ exists in two conformers (A and B) because two $S_1 \leftarrow S_0$ origin bands have been detected at $\nu_A = 37\,534$ and $\nu_B = 37\,583$ cm^{-1} [16]. For each rotational isomer, we have checked the $^{13}C_1$ isotopic selectivity. The laser wavelengths used are $\lambda_{12,A} = 266.36$ nm, $\lambda_{12,B} = 266.01_5$ nm for the R2PI excitation of monoisotopic *n*-propylbenzene, and $\lambda_{13,A} = 266.33$ nm, $\lambda_{13,B} = 265.98$ nm for the R2PI excitation of the $^{13}C_1$-*n*-propylbenzene contained as a natural mixture in the sample. The R2PI induced mass spectrum of conformer A and of conformer B have been found to be identical. Fig. 3 refers to conformer B and displays the R2PI fragmentation pattern of $C_6H_5C_3H_7$ (bottom spectrum, λ_{12}), and of $^{13}CC_5H_5C_3H_7$ (top spectrum, λ_{13}). The major fragment is the *m/z* 91 ($C_7H_7^+$, simple β-cleavage) which is detected at *m/z* 92 in the case of $^{13}CC_5H_5C_3H_7$. The fragmentation pattern of $C_6H_5C_3H_7^{\cdot+}$, Fig. 3(a), includes very weak peaks at *m/z* 105 ($C_8H_9^+$) and 92 ($C_7H_8^+$), indicating that the simple γ-cleavage and the H migration accompanying β-cleavage channels are not important in the ladder switching process in *n*-propylbenzene. The "heavy" *n*-propylbenzene, with the ^{13}C atom outside of the ring, has its maximum absorption coefficient closer to $\lambda_{12,B}$ than to $\lambda_{13,B}$ and these parent ions contribute to the *m/z* = 121 peak present in Fig. 3(a) and 3(b). The fragmentation pattern of $^{13}CC_5H_5C_3H_7^{\cdot+}$ [Fig. 3(b)] shows clearly;

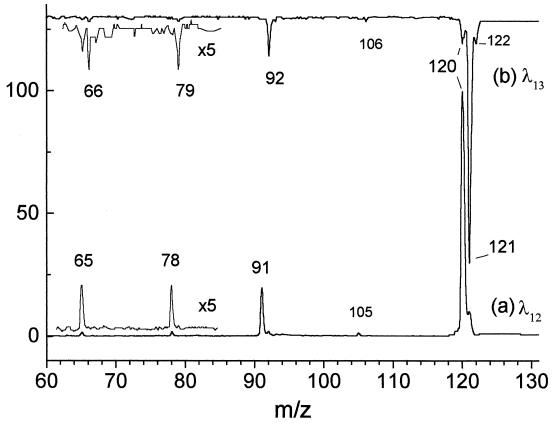

Fig. 3. REMPI mass spectra of *n*-propylbenzene. Parent peaks have been normalized to 100. (a) Laser wavelength tuned at λ_{12}, the $S_1 \leftarrow S_0$ origin band of $C_6H_5C_3H_7$. (b) Laser wavelength tuned at λ_{13}, the $S_1 \leftarrow S_0$ origin band of $^{13}CC_5H_5C_3H_7$.

all the peaks are shifted by 1 Da relative to the fragments of $C_6H_5C_3H_7^{\cdot+}$.

The small peak, *m/z* 122, which appears in Fig. 3(b), is the parent ion with two ^{13}C atoms. The natural isotopic abundance of two ^{13}C atoms in *n*-propylbenzene is 0.4% (for one ^{13}C atom it is ~10%). The intensity of this (A + 2) peak (A stands for the unlabeled molecule) is wavelength dependent having a maximum at ~3 cm^{-1} higher than the wavenumber of the (A + 1) peak. The corresponding (A + 2) peak is also detectable in the other molecules.

3.3. 1,2-Diethylbenzene

The mass-selected supersonic jet cooled $S_1 \leftarrow S_0$ origin region of *ortho*-$C_6H_4(C_2H_5)_2$ has been studied by Breen et al. [28], and a strong origin has been detected at 37 151 cm^{-1}. A weak band, 17 cm^{-1} below this strong origin, has been assigned [28] as the $S_1 \leftarrow S_0$ origin of a second conformer, because its relevant intensity did not change under various expansion conditions. Our spectroscopic investigation agrees with these results. The mass fragmentation patterns induced by R2PI at laser wavelength λ_{12} = 269.15 nm (position of the strong origin) and at λ'_{12} = 269.27 nm (position of the weak origin) are indistinguishable. This result confirms the assignment of the two conformers.

Fig. 4 displays the fragmentation patterns of the *ortho*-diethylbenzene sample induced by R2PI at λ_{12} = 269.15 nm [maximum absorption of $C_6H_4(C_2H_5)_2$] and at λ_{13} = 269.12 nm [maximum absorption of $^{13}CC_5H_4(C_2H_5)_2$].

The prominent fragments of $C_6H_4(C_2H_5)_2$ [Fig. 4(a)] have been observed at *m/z* 119, 105, 91, 77, 79, while weaker peaks appeared at 104, 103, and 78. It is to be noted that in the EI mass spectrum [25], the base peak is the *m/z* 105. In the mass spectrum of Fig. 4(b) the peaks are shifted by 1 Da, relative to the peaks of Fig. 4(a), because the ^{13}C atom is in the ring and remains there. The fragmentation channel $105^+ \rightarrow 79^+ \rightarrow 77^+$ is seen at the $^{13}C_1$ isotopomer as $106^+ \rightarrow (80^+$ and $79^+) \rightarrow (78^+$ and $77^+)$ because the expulsed neutral can be C_2H_2 or $^{13}CCH_2$. This implies that the ejected acetylene comes from the ring.

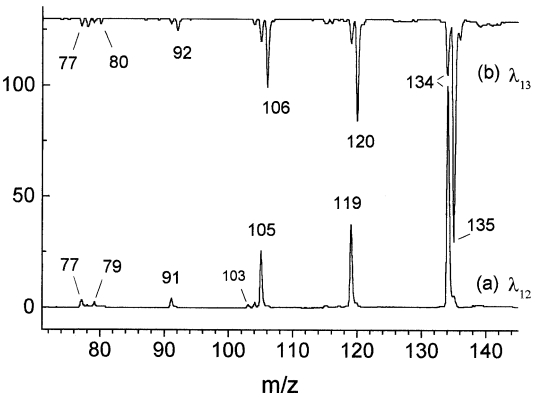

Fig. 4. REMPI mass spectra of *ortho*-diethylbenzene. Parent peaks have been normalized to 100. (a) Laser wavelength tuned at λ_{12}, which corresponds to the $S_1 \leftarrow S_0$ origin band of $C_6H_4(C_2H_5)_2$. (b) Laser wavelength tuned at λ_{13}, which corresponds to the $S_1 \leftarrow S_0$ origin band of $^{13}CC_5H_4(C_2H_5)_2$.

3.4. tert-Butylbenzene

The decomposition of *tert*-butylbenzene molecular ion is dominated by the initial loss of a methyl group (simple bond cleavage) and the expulsion of C_2H_4 from the daughter cation $[C_6H_5(C_3H_6)]^+$ [24,29–31]. The mechanism for the C_2H_4 loss has been of interest because the side-chain carbon atoms in $[C_6H_5(C_3H_6)]^+$ show a degeneracy [24,29–31].

Fig. 5(a) is the R2PI mass selected $S_1 \leftarrow S_0$ origin bands of $C_6H_5C(CH_3)_3$ (dotted line) and of its $^{13}C_1$-isotopomers (solid line), normalized to 10. The maximum of the *m/z* 135 ion signal is at λ_{13} = 265.19 nm and corresponds to the R2PI of $^{13}CC_5H_5C(CH_3)_3$, while the peak that appears on the red side of this envelope, at $\lambda = 265.20_5$ nm, is due to the R2PI of *tert*-butylbenzene with a ^{13}C atom outside of the ring. The unlabeled *tert*-butylbenzene has its maximum absorption at λ_{12} = 265.22 nm. The laser induced fragmentation patterns at wavelengths λ_{12} and λ_{13} are displayed in Fig. 5(b) and 5(c), respectively, and each fragment has been labeled by its *m/z* value. For the fragments with *m/z* ≥ 77 it is clear that the ^{13}C atom is retained in the ring. The *m/z* 41 peak, ($C_3H_5^+$), is common in both patterns (b) and (c) of Fig. 5, indicating that this cation comes from the side chain of $[C_6H_5(C_3H_6)]^+$ and of $[^{13}CC_5H_5(C_3H_6)]^+$, respec-

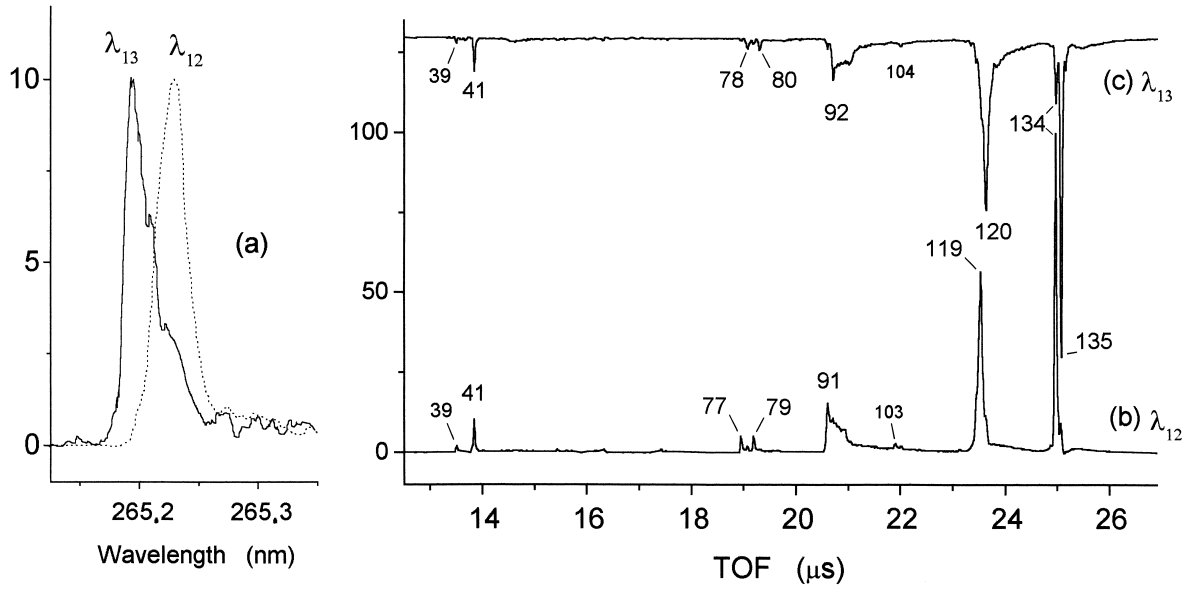

Fig. 5. (a) R2PI mass selected $S_1 \leftarrow S_0$ origin band of jet cooled *t*-butylbenzene (dotted line) and $^{13}C_1$-*t*-butylbenzene (solid line). Both spectra have been scaled to 10. (b) REMPI mass spectrum of *t*-butylbenzene induced by wavelength λ_{12}. (c) REMPI mass spectrum of *t*-butylbenzene induced by wavelength λ_{13}. A non-isotope-enriched sample has been used and the parent peaks have been normalized to 100. The horizontal axis is the time-of-flight of the fragments and it was not converted to the *m/z* values, because of the special shapes of the *m/z* 91, 119 [in (b)] and *m/z* 92, 120 [in (c)] peaks.

tively. Also, most of the *m/z* 39 ions do not have a ^{13}C atom. The shape of the *m/z* 91 and 119 peaks (92 and 120 for the $^{13}C_1$-isotopomer) deserves further comments. The broadness of the *m/z* 119 peak [Fig. 5(b)] is due to the dissociation of this ion in the field-free region with kinetic energy release. The metastable shape of the *m/z* 91 signal is interpreted as due to the *m/z* 119 → 91 collision-induced dissociation in the ionization-draw-out region of the TOF mass spectrometer. By increasing the sample concentration, the *m/z* 119 ion interacts with the neutral parent molecule and gives a new ion with *m/z* 121. This is faintly seen in Fig. 5(b), close to 23.9 μs. A complete study of these features will be given in a forthcoming report.

4. Conclusions

Using non-isotope-enriched samples, it is demonstrated that REMPI mass spectrometry can be used to observe the fragments of the $^{13}C_1$ labeled molecules, which are present in natural abundance, and to almost eliminate these fragments from the fragmentation pattern of the main molecule by tuning the laser to appropriate wavelengths. Fragmentation mechanisms are not completely clear from the comparison of these mass spectra because such studies mostly rely on labeling in known positions. However, the method permits the use of synthetically prepared compounds of low concentration in the labeled position. It will be perfectly effective in deuterium labeled compounds because substitution of a ^1H atom by ^2H has a much larger isotopic shift in the molecular vibronic transition than the substitution of a ^{12}C atom by ^{13}C. The quality of the mass spectrum can be further improved by introducing a second dye laser for the photodepletion (hole burning) of the unwanted molecules. In such an experiment, the excitation/ionization laser has to be at $\lambda_{labeled}$ and the depletion laser at $\lambda_{unlabeled}$ in order to get the fragmentation pattern of the labeled molecule. The potential of the laser hole burning

technique has been documented in other areas of spectroscopy; for example, in the discrimination of rotational isomers [32,33] and dimers [34].

Acknowledgement

The authors would like to acknowledge Dr. D. Kuck, University of Bielefeld, for critically reading the manuscript.

References

[1] V.A. Antonov, I.N. Knyazev, V.S. Letokhov, V.M. Matiuk, V.G. Movshev, V.K. Potapov, Opt. Lett. 3 (1978) 37; Pis'ma Zh. Tekh. Fiz. 3 (1977) 1287.
[2] U. Boesl, H.J. Neusser, E.W. Schlag, Z. Naturforsch. Teil A 33 (1978) 1546.
[3] L. Zandee, R.B. Bernstein, D.A. Lichtin, J. Chem. Phys. 69 (1978) 3247.
[4] S. Rockwood, J. Reilly, K. Hohla, K.L. Kompa, Opt. Commun. 28 (1979) 175.
[5] D.M. Lubman, R. Naaman, R.N. Zare, J. Chem. Phys. 72 (1980) 3034.
[6] U. Boesl, H.J. Neusser, E.W. Schlag, J. Chem. Phys. 72 (1980) 4327.
[7] T.G. Dietz, M.A. Duncan, M.G. Liverman, R.E. Smalley, J. Chem. Phys. 73 (1980) 4816.
[8] H.J. Neusser, Int. J. Mass Spectrom. Ion Phys. 79 (1987) 141.
[9] D.M. Lubman, Anal. Chem. 59 (1987) 31A.
[10] J. Grotemeyer, E.W. Schlag, Angew. Chem. Int. Ed. Engl. 27 (1988) 447.
[11] U. Boesl, J. Phys. Chem. 95 (1991) 2949.
[12] P.M. Johnson, C.E. Otis, Ann. Rev. Phys. Chem. 32 (1981) 139.
[13] U. Boesl, H.J. Neusser, E.W. Schlag, J. Am. Chem. Soc. 103 (1981) 5058.
[14] R. Tembreull, C.H. Sin, P. Li, H.M. Pang, D.M. Lubman, Anal. Chem. 57 (1985) 1186.
[15] K.G. Owens, J.P. Reilly, J. Opt. Soc. Am. B 2 (1985) 1589.
[16] P.J. Breen, J.A. Warren, E.R. Bernstein, J.I. Seeman, J. Chem. Phys. 87 (1987) 1927.
[17] A. de la Cruz, M. Ortiz, J.A. Cabrera, J. Campos, Int. J. Mass Spectrom. Ion Phys. 133 (1994) 39.
[18] O. Dimopoulou-Rademann, K. Rademann, B. Brutschy, H. Baumgärtel, Chem. Phys. Lett. 101 (1983) 485.
[19] S. Leutwyler, U. Even, Chem. Phys. Lett. 81 (1981) 578.
[20] D.M. Lubman, R. Tembreull, C.H. Sin, Anal. Chem. 57 (1985) 1084.
[21] W. Dietz, H.J. Neusser, U. Boesl, E.W. Schlag, S.H. Lin, Chem. Phys. 66 (1982) 105.
[22] S. Meyerson, P.N. Rylander, J. Chem. Phys. 27 (1957) 901.
[23] K.L. Rinehart, A.C. Buchholz, G.E. Van Lear, H.L. Cantrill, J. Am. Chem. Soc. 90 (1968) 2983.
[24] D. Kuck, Mass Spectr. Rev. 9 (1990) 187.
[25] NIST Standart Reference Database 69-March 1998, http://webbook.nist.gov/chemistry
[26] C. Kosmidis, J.G. Philis, Int. J. Mass Spectrom. Ion Processes 173 (1998) 143.
[27] J.G. Philis, C. Kosmidis, Int. J. Quantum Chem. 72 (1999) 341.
[28] P.J. Breen, E.R. Bernstein, J.I. Seeman, J. Chem. Phys. 87 (1987) 3269.
[29] P.N. Rylander, S. Meyerson, J. Am. Chem. Soc. 78 (1956) 5799.
[30] S. Meyerson, H. Hart, J. Am. Chem. Soc. 85 (1963) 2358.
[31] R. Neeter, N.M.M. Nibbering, Org. Mass Spectrom. 7 (1973) 1091.
[32] R.J. Lipert, S.D. Colson, J. Phys. Chem. 93 (1989) 3894.
[33] T. Bürgi, S. Leutwyler, J. Chem. Phys. 101 (1994) 8418.
[34] W. Scherzer, O. Krätschmar, H.L. Selzle, E.W. Schlag, Z. Naturforsch 47a (1992) 1248.